# Identification of deliberate catheter motion at the left atrial posterior wall during pulmonary vein isolation: Validity of respiratory motion adjustment

Tomlinson, DR; Biscombe, K; True, J; Hosking, J; Streeter, AJ

**Published in:**
Journal of Cardiovascular Electrophysiology

**DOI:**
10.1111/jce.14945

**Publication date:**
2021

# Detection of catheter displacement during contact force and VISITAG™ Module-guided pulmonary vein isolation: An improved approach towards respiratory adjustment


Authors: David R. Tomlinson BM BSc MD[1], Katie Biscombe[2], John True BSc MSc[2], Joanne Hosking BSc PhD[2] and Adam Streeter MSc PhD[2]

Corresponding address: [1]University Hospitals Plymouth NHS Trust, South West Cardiothoracic Centre, Derriford Hospital, Plymouth, UK, PL6 8DH

[2]Department of Medical Statistics, Plymouth University Peninsula Schools of Medicine and Dentistry, ITTC Building 1, Plymouth Science Park, Plymouth, Devon PL6 8BX, UK.

Tel: 01752 431838

Email: david.tomlinson1@nhs.net


Word count: Abstract 250; body text 3931; references 771

## Abstract

### Background

During automated radiofrequency (RF) annotation-guided pulmonary vein isolation (PVI), respiratory motion adjustment (RMA) is recommended, yet lacks in vivo validation.

### Methods

Following contact force (CF) PVI (continuous RF, 30 W) using general anesthesia and automated RF annotation-guidance (VISITAG™: force-over-time 100% minimum 1 g; 2 mm position stability; ACCURESP™ RMA "off") in 25 patients, we retrospectively examined RMA settings "on" versus "off" at the left atrial posterior wall (LAPW).

### Results

Respiratory motion detection occurred in eight, permitting offline retrospective comparison of RMA settings. Significant differences in LAPW RF auto-annotation occurred according to RMA setting, with curves displaying catheter position, CF and impedance data indicating "best-fit" for catheter motion detection using RMA "off." Comparing RMA "on" versus "off," respectively: total annotated sites, 82 versus 98; median RF duration per-site, 13.3 versus 10.6 s ($p < 0.0001$); median force time integral 177 versus 130 gs ($p = 0.0002$); mean inter-tag distance (ITD), 6.0 versus 4.8 mm ($p = 0.002$). Considering LAPW annotated site 1-to-2 transitions resulting from deliberate catheter movement, 3 concurrent with inadvertent 0 g CF demonstrated < 0.6 s difference in RF duration. However, 13 deliberate catheter movements during constant tissue contact (ITD range: 2.1–7.0 mm) demonstrated (mean) site-1 RF duration difference 3.7 s (range: −1.3 to 11.3 s): considering multiple measures of catheter position instability, the appropriate indication of deliberate catheter motion occurred with RMA "off" in all.

### Conclusions

ACCURESP™ respiratory motion adjustment importantly delayed the identification of deliberate and clinically relevant catheter motion during LAPW RF delivery, rendering auto-annotated RF display invalid. Operators seeking greater accuracy during auto-annotated RF delivery should avoid RMA use.

## Keywords

Atrial fibrillation; contact force catheter ablation; pulmonary vein isolation; ACCURESP™ Module; VISITAG™ Module

## Introduction

The central importance of electrical isolation of the pulmonary veins (PVs) towards eliminating atrial fibrillation (AF) is well-established[1,2], but achieving this end-point using catheter ablation involves three principal challenges: (1) There is no universally applicable and validated means to directly visualise ablation lesion creation, either in terms of the transmural (TM) extent or radius; (2) The left atrial (LA) wall thickness is variable[3], yet unknown to the operator, and while partial wall-thickness lesions result in electrical

conduction gaps and recurrent AF[2,4], excessive energy delivery risks life-threatening extra-cardiac thermal trauma[5], and; (3) Cardiac and respiratory cycle-induced motion creates a moving target for radiofrequency (RF)-based catheter ablation technologies.

Theoretically, idealised pulmonary vein isolation (PVI) protocols are likely to involve variable energy dosing according to the LA wall thickness, with real-time incorporation of suitable measures of the tissue effects of energy delivery – i.e. lesion transmurality and radius – into a 3D "model" using objective and validated methods. When supported by suitable methodology for defining a stable point of catheter-tissue interaction during RF application, such "modelling" should facilitate the knowing completion of permanent PVI, without extra-cardiac thermal trauma, in all but exceptional cases and for all suitably skilled operators.

Important progress towards this goal has been reported in studies utilising the objective RF annotation module VISITAG™ (Biosense Webster Inc., Diamond Bar, CA), with a coordinated series of methodological steps towards tailored contact force (CF)-guided PVI lesion sets, including targeting minimum permissible inter-lesion distance (ILD) and site-specific RF energy delivery (i.e. anterior versus posterior wall) according to a weighted formula incorporating measures of RF power, duration and CF.[6,7] However, although very high clinical success has been achieved in selected operators' practice, these protocols fail to represent perfect descriptors of reproducible and suitably tailored PVI protocols in four important respects: (1) Studies of RF delivery during PVI in humans have provided evidence of greater effect at left-sided LA posterior wall (LAPW) sites[8,9], therefore any protocol without suitable energy dosing adjustment is likely to incur increased risk of extra-cardiac thermal trauma; (2) There was no incorporation of measures of the TM tissue response to RF delivery, yet *in vivo* animal studies have demonstrated that a change in the unipolar

electrogram (UE) morphology from RS to "pure R" may be indicative of histologically-confirmed TM lesions.[10,11] Furthermore, a study conducted in humans has confirmed the utility of RF titration according to real-time assessments of pure R UE morphology change towards a highly effective CF-guided PVI protocol[12]; (3) The chosen VISITAG™ Module CF filter settings (force-over-time 30%, minimum 5g[13] and 30% minimum 4g[7]) permit variable out-of-phase catheter-tissue interaction due to intermittent catheter-tissue contact (i.e. 0g CF), though with RF annotation on-going and displayed / modelled as a single point; (4) Employing either conscious sedation or general anaesthesia (GA) with intermittent positive pressure ventilation (IPPV), these studies routinely utilised ACCURESP™ respiratory adjustment (Biosense Webster) "on" for VISITAG™ Module annotation (Molloy Das, personal communication). However, ACCURESP™ remains without *in vivo* validation as a component of automated RF annotation and lesion modelling methodology.

Therefore, the purpose of this present report was to retrospectively investigate the effects of ACCURESP™ respiratory adjustment setting on RF lesion modelling using the VISITAG™ Module, thereby determining the most appropriate ACCURESP™ setting for RF lesion annotation during CF and VISITAG™ Module-guided PVI.

## Methods

CF and VISITAG™ Module-guided PVI was performed by a single-operator employing a previously reported standardised protocol[9] in a consecutive series of unselected adult patients with symptomatic AF undergoing first-time PVI according to current treatment indications.[14] Briefly, all procedures were undertaken using GA and IPPV, with ACCURESP™ respiratory training undertaken pre-ablation and applied as required to complete the CARTO®3 geometry (V.3, Biosense Webster). Specifically, ACCURESP™ training was first performed with a

LASSO®Nav catheter (Biosense Webster, 2-5-2mm inter-electrode spacing) placed in the right superior PV. If there was insufficient respiratory motion to trigger the ACCURESP™ detection threshold, the catheter was placed in the left inferior PV and ACCURESP™ training re-checked. The tidal volume was never deliberately increased, so ACCURESP™ respiratory motion detection was negative in some cases. Importantly, even in cases where the ACCURESP™ respiratory adjustment threshold was triggered, the ACCURESP™ setting "on" was never prospectively applied to the VISITAG™ Module filter preferences during ablation.

Temperature-controlled RF at 30W (17ml/min irrigation) was delivered via a ThermoCool® SmartTouch® catheter using Agilis™ NxT sheath (Abbott, St Paul, MN) support during proximal pole CS pacing at 600ms. VISITAG™ Module filter preferences for automated RF annotation were: Positional stability range 2mm, tag display duration 3s; force-over-time 100% minimum 1g (the latter derived from a previous study[15] and designed to ensure per-site RF annotation only in the presence of constant catheter-tissue contact). Lesion placement was guided by VISITAG™ Module annotation, with the preferred site of first RF application at the LAPW opposite each superior PV ~1cm from the PV ostium; in cases where constant catheter-tissue contact could only be achieved with maximal CF ≥70g, an adjacent LAPW site with lower peak CF was chosen. The target annotated RF duration at each first-ablated LAPW site, as well as any subsequent "RF ON" sites and the carina (if ablated) was 15s, whereas ~9-11s was the target for all other sites consecutively annotated during continuous RF delivery. Following the required period of first-site annotated RF, target ILD ≤6mm was achieved predominantly during continuous RF application using rapid movement of the catheter tip initiated via the Agilis sheath, aided by the distance measurement tool; point-by-point RF was also applied as necessary. Following completion of circumferential PVI (entrance and exit block), spontaneous recovery of PV conduction was assessed and

eliminated during a minimum 20-minute wait; dormant recovery was evaluated and eliminated a minimum of 20 minutes after the last RF. Neither oesophageal luminal temperature monitoring nor post-ablation endoscopic evaluation was employed.

For all cases where ACCURESP™ triggering threshold was exceeded, VISITAG™ Module annotated RF and UE morphology change data were retrospectively collected. The focus for analysis was all ablation-naïve LAPW sites (i.e. first encirclement, not including touch-up lesions), since ablation here entails risk of atrio-oesophageal fistula (AEF) and therefore accurate lesion modelling via automated annotation methodology is of particular importance. Annotated RF duration, mean CF, force time integral (FTI) and impedance drop data for each site were obtained via the VISITAG™ Module export function; to examine the effects of ACCURESP™ setting, data export was performed separately for ACCURESP™ "on and "off". ILD was determined on-line using the proprietary measurement tool. Retrospective UE analysis was performed via CARTOREPLAY™ (Biosense Webster) as previously described[9]; electrograms are automatically deleted at 12-18 hours after case completion (a CARTO®3 system function), so UE morphology data was only obtained for the ACCURESP™ "off" setting.

For all data exports, R software code[16] was used to analyse the catheter tip position, measured at a rate of 60 positions (x, y, z coordinates) per second; the "RawPositions" data file was used for this purpose since this represents the "unadjusted" (for respiratory motion; i.e. "true") catheter tip position. Suitable code was used to calculate a rolling standard deviation (SD) of the Euclidian distances shifted between each position over a one second period, the same settings used to determine stability by the CARTO®3 system logic. These "position stability" data were plotted according to the patient interface unit (PIU) "system" time. These were supplemented with the absolute CF (at 20Hz) and impedance (at 10Hz) data derived from the exported "ContactForceData" "AblationData" files respectively, and end-expiration

timing data from the "EndExperium" file. Finally, PIU start and stop times for annotated sites according to each ACCURESP™ setting were obtained from exported "AblationSites" files.

**Statistical analysis plan**

Exported text files were converted to Excel data suitable for analysis and copied to GraphPad Prism version 4.03 (GraphPad Software, San Diego, CA). Normality testing was performed; parametric data are expressed as mean [standard deviation, SD] and non-parametric data as median (1st – 3rd quartile). The initial question was whether ACCURESP "on" versus "off" settings resulted in significant differences in the number of annotated LAPW sites, annotated RF duration, ILD, total impedance drop, mean CF and FTI. Following this, ACCURESP "on" versus "off" annotation performance was assessed at sites of known (deliberate) catheter position instability at transition between the first and second-annotated sites. Unpaired / paired t test, Mann Whitney / Wilcoxon signed rank tests were used to assess statistical significance for continuous data, as appropriate. $P < 0.05$ indicated a statistically significant difference. This work received IRB approval for publication as a retrospective service evaluation; all patients provided written, informed consent.

## Results

Twenty-five patients underwent first-time PVI as described, between November 2016 and May 2017: 13 persistent AF, 12 PAF; 19 male (76%); age 57 [14] years and $CHA_2DS_2$-VASc score 1.3 [1.3]. Complete PVI was achieved in all without spontaneous / dormant recovery of PV conduction, following 16.2 [3.1] minutes of RF, with no procedural complications. The ACCURESP™-triggering cohort comprised 8 of 25 cases (32%); considering age, body mass

index and RF duration required for case completion, there were no significant differences with the cohort without ACCURESP™ threshold triggering.

Comparing ACCURESP™ "on" with "off", the number of annotated LAPW sites and total LAPW RF duration were 82 and 98, and 1091s and 1006s, respectively (annotated biophysical RF data according to ACCURESP™ setting are shown in table 1). For each group of annotated sites (i.e. left or right-sided), per-site RF duration and FTI were significantly greater with ACCURESP™ "on" versus "off"; i.e. left-sided RF duration 13.1s versus 9.9s (p=0.0003) and FTI 156g.s versus 114g.s (p=0.0003), respectively and right-sided RF duration 13.5s versus 10.6s (p=0.006) and FTI 228g.s versus 166g.s (p=0.04), respectively. Combined data analysis also demonstrated significantly greater ILD with ACCURESP™ "on"; i.e. 6.0mm versus 4.8mm (p=0.002). A comparison of annotated biophysical data at first-annotated sites according to ACCURESP™ setting is shown in table 2; combined data analysis demonstrated that per-site RF duration, impedance drop, FTI and ILD were all significantly greater with ACCURESP™ "on" versus "off".

**Analyses at sites of deliberate catheter movement: Site 1 to 2 transition**

Annotated biophysical data according to ACCURESP™ setting were analysed at sites of deliberate catheter motion between annotated sites 1 and 2. Movement was defined by either: (1) Site 1 annotation "end" due to a 0g CF event (i.e. CF breaching the VISITAG™ Module force-over-time filter of 100% minimum 1g), or; (2) Inter-ablation site transition accompanied by UE morphology change from pure R at site 1 completion, to RS at site 2 onset (i.e. indicating movement from a site of TM ablation effect to an adjacent ablation naive site). Comparison of annotated biophysical data (ACCURESP™ "on" minus "off") at 3 sites of position instability according to a 0g CF event demonstrated maximal difference in

annotated RF duration, FTI and ILD of -0.6s, -17g.s and 2.2mm respectively, with no difference in annotated impedance drop (table 3 and figures 1-3). However, comparison (ACCURESP™ "on" minus "off") at 4 ablation site transitions associated with UE morphology change from pure R (site 1 completion) to RS (site 2 onset) demonstrated maximal difference in RF duration, FTI, ILD and impedance drop of 11.3s, 139g.s, 2.6mm and 3.3Ω respectively (table 3 and figures 4-7), with the first indication of catheter movement represented by ACCURESP™ "off" annotation in all cases. The greatest difference was seen in a case where the site 1 to 2 ILD with ACCURESP™ "off" was 4.1mm (reconstituted data curves, figure 4); at 15.2s following RF onset there was an abrupt increase in catheter position shift and SD, with a corresponding change in CF waveform, yet while the blue vertical line indicating annotation site transition according to ACCURESP™ set "off" coincided with these changes and the "per protocol" 15s RF at site 1, the red vertical line indicating annotated site transition using ACCURESP™ set "on" can be seen 11.3s later.

**Analyses at remaining site 1 to 2 transitions**

Catheter movement at 9 site 1 to 2 transitions occurred with CF ≥1g and continuous pure R UE morphology – i.e. at site 1 end and immediately at site 2 onset. Comparison of annotated biophysical data (ACCURESP™ "on" minus "off") demonstrated a difference in RF duration of <1s in 1 case (table 1, data supplement); in 8/9 the difference in annotated RF duration was ≥1s (range -1.3 – 8.6s, mean 3.7 [4.0] s). The maximum difference in RF duration, FTI, ILD and impedance drop were 8.6s, 208g.s, 7.7mm and 1.4Ω respectively, with ACCURESP™ "on" resulting in greater values for annotated data in 7/9 (table 1, data supplement). Considering multiple measures of catheter position stability, the first indication of catheter motion was appropriately indicated using ACCURESP™ "off" in 8/9; only one case

demonstrated no significant difference in annotation timing (i.e. 0.1s, supplementary figure 9).

In the 13 site 1 to 2 transitions achieved with constant catheter-tissue contact, the relationship between differences in annotated RF data (ACCURESP™ "on" minus "off") and ILD (with ACCURESP™ "off") is shown in figure 8. There was a significant negative correlation between the difference in annotated RF duration and ILD – Pearson r -0.68 (95% confidence interval -0.91 to -0.13, p=0.02, supplementary figure 1). Therefore, while the maximal difference in annotated RF duration with site 1 to 2 ILD ≥6mm was 1.1s, an ILD ≤5mm was associated with maximal difference in annotated RF duration of 11.3s. Data supplement figures 2 – 10 demonstrate all remaining annotated site 1 to 2 transitions, with corresponding position shift, SD, CF and impedance data.

**Analyses at annotated LAPW sites during subsequent continuous RF application**

All left-sided LAPW lesion sets and 6 of 8 right-sided LAPW lesion sets were completed during continuous RF application; the onset timing of transitions for sites 2 to 5 is shown in table 4. For left-sided LAPW lesions there was a progressively greater difference between annotated site transition timings with ACCURESP "on" versus "off", increasing from 1.2s (0.4 – 5.0) at site 2 onset, to 14.6s (7.6 – 23.0) at site 5 annotation onset; an example is shown in supplementary figures 11-14, with annotated position shift, SD, CF and impedance data.

## Discussion

The main findings of this present study are as follows: (1) ACCURESP™ respiratory adjustment results in important differences in VISITAG™ Module annotation at the LAPW, with ACCURESP™ set "on" overall resulting in significantly greater per-site RF duration and ILD; (2) At sites of deliberate catheter motion between first and second-annotated sites

effected without loss of catheter-tissue contact, annotated transition using ACCURESP™ "off" demonstrated suitable accuracy towards catheter motion detection and inter-ablation site transition annotation in all cases. However, ACCURESP™ "on" resulted in inappropriate annotation delay of ≥1s in the majority (i.e. 9/13); (3) ACCURESP™ setting was only without significant effect on RF annotation when sites of deliberate catheter motion were accompanied by loss of catheter-tissue contact (i.e. 0g CF) and while using a force-over-time filter of 100% minimum 1g; (4) There was a significant inverse relationship between the difference in first-annotated site RF duration (ACCURESP™ "on" minus "off"), and the ACCURESP™ "off" site 1 to 2 ILD. Consequently, with ACCURESP™ "on", catheter tip motion of up to 7mm was not immediately identified, resulting in delayed annotation of site 2 onset and consequent error in per-site RF parameters. More simply, ACCURESP "on" may effectively render an operator "blind" to the immediate occurrence of small but clinically important catheter displacement events.

These results may be better understood when considering the VISITAG™ Module annotation "system logic" and how this is modified by ACCURESP™ use. Briefly, the ablation catheter tip position is measured in a "rolling window" of 60 sites per second (i.e. intervals of 16/17ms), from which is calculated the standard deviation (SD). With ACCURESP™ "off", RF annotation occurs when both every second of position data is within twice (2x) the user-defined position SD, and a total consecutive minimum of 3s is within (1x) the SD. However, with ACCURESP™ "on", the position stability filter operates over a minimum of two respiratory cycles, using position data "adjusted" to end-expiration; here, automated ablation site annotation occurs when these position stability targets are met *following data adjustment*. Importantly, annotation only occurs when CF filter preferences are also satisfied. However, in contrast to position stability filtering, the CF filter is applied continuously regardless of

ACCURESP™ setting (i.e. independent of the respiratory cycle). Therefore, with the force-over-time 100% minimum 1g CF filter used during this present report, RF annotation "end" logic is fulfilled by any 0g CF event at any stage in the respiratory cycle, with ACCURESP™ both "on" and "off".

**Importance of these findings: Historical perspective**

Following the advent of VISITAG™ Module automated RF annotation, this tool has been demonstrated to facilitate both the derivation of hypothetically ideal per-site ablation parameters and their subsequent delivery during CF and VISITAG™ Module-guided PVI.[6,7,13,15] Such targets can only be considered appropriate when "derivation phase" methodology employed a suitable definition for a stable site of catheter-tissue interaction during RF application. Notwithstanding the theoretical difficulty resulting from a choice of CF filter permitting intermittent catheter-tissue contact (i.e. by definition a stable site can only occur in the setting of constant tissue contact), the foundational study supporting a regional difference in ablation target values also used ACCURESP™ "on" in all cases; procedures performed under GA and with IPPV failing to trigger ACCURESP™ had the tidal volume increased to ensure ACCURESP™ triggering and "on" setting use (Molloy Das, personal communication).[13] As this present report has demonstrated that catheter tip movements of up to 7mm are not immediately identified with ACCURESP™ "on", these previously identified ablation targets are likely to be importantly flawed.

**Clinical importance in light of novel high power, short per-site RF duration protocols**

RF lesion formation occurs more rapidly at higher power.[17] Recently reported high power short duration (HPSD) protocols (50W, typically ~5s per site)[18,19] are particularly attractive for operators wishing to move away from the requirement to maintain a stable catheter position for the ~20-40s previously considered necessary to achieve TM RF effect during

PVI.[1,20] A greater rate of lesion formation means HPSD protocols are particularly dependent upon suitable methodology towards the immediate and accurate determination of clinically relevant catheter position instability. However, to our knowledge no HPSD manuscript includes details of whether respiratory adjustment was applied to RF annotation logic. Alongside the recommendation from Biosense Webster for routine VISITAG™ Module use with ACCURESP™ "on", this calls into question the validity of such HPSD "per-site" ablation targets (since they were likely to have been performed using RF annotation with respiratory adjustment) and whether present HPSD protocols may be considered reproducible.

**Future directions for research**

For VISITAG™ Module-guided procedures, the other important determinant of RF annotation logic towards a suitable definition of a stable site of catheter tissue interaction during RF application is the choice of position stability filter setting. Indeed, a possible solution to the inaccuracy of ACCURESP™ "on" as described in this present report is to use a smaller position stability filter range – e.g. 1.5mm. Although a complete description of the effects of this position filter setting is beyond the scope of this present report, data supplement figure 15 demonstrates annotated left PV site 1 data for case #5 (reconstituted data curves in figure 4), using the VISITAG™ Module preference settings ACCURESP™ "off" with 2mm position stability, and ACCURESP™ "on" with 1.5mm position stability. Importantly, when using 1.5mm stability with ACCURESP™ "on", site 1 annotated RF duration is 1.6s greater, yet as shown in figure 4, position stability and CF changes indicating first catheter displacement coincide with annotation using ACCURESP™ "off" (blue vertical line). In this case, further evidence towards this earlier time point represented the "true" site of catheter displacement is provided by the UE morphology change from pure R (site 1 end)

to RS (site 2 onset). A delay of 1.6s is likely to be clinically important, particularly when considering HPSD ablation.

Together with a steerable sheath for catheter support, high frequency jet ventilation (HFJV) has been shown to reduce the occurrence of acute and chronic pulmonary vein reconnections as well as improve freedom from AF.[21] Theoretically, absence of respiratory motion not only eliminates the requirement for respiratory adjustment, but also confers the advantage of eliminating a requirement for adjustments to sheath and/or catheter position according to the respiratory cycle; presently, there is no means to capture data on such patient and/or operator-specific movements. Accordingly, VISITAG™ Module and CF-guided PVI protocols using HFJV may demonstrate greater reproducibility and efficacy.

**Limitations**

This report was of a single operator's practice, with analyses limited to LAPW lesions in view of the risk of atrio-oesophageal fistula resulting from excessive RF application at this site. It is possible that ACCURESP™ settings demonstrate greater annotation concordance at alternative left atrial sites; such analyses were beyond the scope of this present report. The personalised VISITAG™ Module filter preferences (force-over-time 100% minimum 1g, with 2mm position stability), overdrive atrial pacing and steerable sheath use towards achieving catheter stability and optimal ILD during continuous RF application must be taken into account when considering these experimental findings. If the more commonly employed force-over-time 30% minimum 4-5g CF filter was employed[7,13], intermittent catheter-tissue contact would only trigger per-site annotation "end" if position data breached the chosen (position) stability criteria at that time-point. We elected not to perform a complete re-analysis of exported data with this different CF filter setting, since a site of stable catheter-

tissue interaction during RF by definition may only occur in the setting of constant catheter-tissue contact (i.e. assuming no catheter CF measurement error, force-over-time 100% ≥1g). Also, a complete description of the effects of changing the position stability filter setting is beyond the scope of this present report; this will be the subject of a future manuscript.

Catheter tip motion characteristics following deliberate movement may importantly differ from unintentional events; due to the very high attainment of target per-site RF delivery in this present report, a description of position stability, CF and impedance profiles at sites of accidental catheter motion is beyond the scope of this present report. However, when deliberate catheter displacement events of up to ~5-7mm were not immediately identified when using annotation with ACCURESP™ "on", similar degrees of movement during unintentional catheter displacement events are likely to be missed.

The findings of this present report can only be directly applied to VISITAG™ Module-guided PVI. However, EnSite Precision™ (Abbott) – the only other system with an automated RF annotation module, AutoMark™ – routinely applies respiratory "compensation" to catheter position data. Accordingly, these present findings may have important implications for the methodological rigour of AutoMark™-based RF annotation; at the very least, further studies are warranted to investigate the accuracy and reproducibility of this technology.

It remains impossible to determine the site-specific magnitude of any out-of-phase catheter tissue interaction occurring during constant contact using the methodology described in this present report; intra-cardiac echo was never used. Therefore, even with ACCURESP™ "off", respiratory motion may represent an important determinant of the recently identified heterogeneity in RF effect during PVI.[9,22,23] Furthermore, cardiac cycle-induced motion may

represent another important determinant of catheter instability, although atrial overdrive pacing during RF delivery has been demonstrated to improve catheter stability and impedance reduction;[24] this technique was also used in this present report.

Finally, this report is based on analyses of 8 PVI procedures from a total cohort of 25 patients – i.e. a small sample size from which to conventionally derive meaningful data. However, RF annotation-guided ablation represents a very "data-rich" operative environment and analyses for each ~15s first-site RF application alone utilise 3090 exported data points (i.e. CF at 20Hz, impedance at 10Hz, and both position SD and position shift at 60Hz). Therefore, although drawn from an 8-patient cohort, the findings of this present report represent a total analysis of ~165,000 data points.

**Conclusions**

During CF and VISITAG™ Module annotation-guided PVI, ACCURESP™ respiratory adjustment results in importantly delayed identification of deliberate catheter motion of up to 5-7mm. Accordingly, previously derived ablation targets employing ACCURESP™ "on" may be importantly flawed, and on-going respiratory adjustment use is likely to represent an important impediment towards greater procedural reproducibility, efficacy and safety. In contrast, RF annotation with ACCURESP™ "off" demonstrated excellent catheter motion detection capabilities. Based on these findings, our recommendation is for ACCURESP™ "off" to be the standard approach to VISITAG™ Module use during CF-guided PVI.

## Acknowledgements

I am grateful to Cherith Wood, Daniel Newcomb and Ian Lines, Cardiac Physiologists, for their technical support into all cases conducted during this report. I am also grateful to

Robert Pearce and Vicky Healey (Biosense Webster Inc.) for additional technical assistance and to Noam Seker-Gafni, Tal Bar-on, Einav Geffen, Assaf Rubissa and colleagues at the Haifa Technology Center, Israel for their help with VISITAG™ Module technical queries.

## Sources of Funding

I am grateful to the "Sarkar Research and Training" charitable fund, University Hospitals Plymouth NHS Trust for a donation of £1000, funding the R software code development and extended data analyses by teams at the Department of Medical Statistics, Plymouth University Peninsula Schools of Medicine and Dentistry.

## Disclosures

None

## References

1. Pappone C, Rosanio S, Oreto G, et al. Circumferential radiofrequency ablation of pulmonary vein ostia: A new anatomic approach for curing atrial fibrillation. *Circulation*. 2000;102(21):2619-2628. http://www.ncbi.nlm.nih.gov/pubmed/11085966. Accessed November 20, 2017.
2. Ouyang F, Antz M, Ernst S, et al. Recovered pulmonary vein conduction as a

dominant factor for recurrent atrial tachyarrhythmias after complete circular isolation of the pulmonary veins: lessons from double Lasso technique. *Circulation*. 2005;111(2):127-135. doi:10.1161/01.CIR.0000151289.73085.36.

3. Beinart R, Abbara S, Blum A, et al. Left atrial wall thickness variability measured by CT scans in patients undergoing pulmonary vein isolation. *J Cardiovasc Electrophysiol*. 2011;22(11):1232-1236.
4. Badger TJ, Daccarett M, Akoum NW, et al. Evaluation of left atrial lesions after initial and repeat atrial fibrillation ablation: lessons learned from delayed-enhancement MRI in repeat ablation procedures. *Circ Arrhythm Electrophysiol*. 2010;3(3):249-259. doi:10.1161/CIRCEP.109.868356.
5. Black-Maier E, Pokorney SD, Barnett AS, et al. Risk of atrioesophageal fistula formation with contact force–sensing catheters. *Heart Rhythm*. 2017;14(9):1328-1333. doi:10.1016/j.hrthm.2017.04.024.
6. Hussein A, Das M, Chaturvedi V, et al. Prospective use of Ablation Index targets improves clinical outcomes following ablation for atrial fibrillation. *J Cardiovasc Electrophysiol*. 2017;28(9):1037-1047. doi:10.1111/jce.13281.
7. Taghji P, El Haddad M, Phlips T, et al. Evaluation of a Strategy Aiming to Enclose the Pulmonary Veins With Contiguous and Optimized Radiofrequency Lesions in Paroxysmal Atrial Fibrillation: A Pilot Study. *JACC Clin Electrophysiol*. 2018;4(1):99-108. doi:10.1016/j.jacep.2017.06.023.
8. Knecht S, Reichlin T, Pavlovic N, et al. Contact force and impedance decrease during ablation depends on catheter location and orientation: insights from pulmonary vein isolation using a contact force-sensing catheter. *J Interv Card Electrophysiol*. 2015;43(3):297-306. doi:10.1007/s10840-015-0002-8.
9. Tomlinson D, Myles M, Stevens K, Streeter AJ. Transmural unipolar electrogram

morphology is achieved within 7s at the posterior left atrial wall during pulmonary vein isolation: VISITAG™ Module-based lesion assessment during radiofrequency ablation. *bioRxiv*. December 2017:234799. doi:10.1101/234799.

10. Otomo K, Uno K, Fujiwara H, Isobe M IY. Local unipolar and bipolar electrogram criteria for evaluating the transmurality of atrial ablation lesins at different catheter orientations relative to the endicardial surface. *Heart Rhythm*. 2010;7(9):1291-1300.
11. Bortone A, Brault-Noble G, Appetiti A, Marijon E. Elimination of the negative component of the unipolar atrial electrogram as an in vivo marker of transmural lesion creation: acute study in canines. *Circ Arrhythm Electrophysiol*. 2015;8(4):905-911. doi:10.1161/CIRCEP.115.002894.
12. Bortone A, Lagrange P, Cauchemez B, et al. Elimination of the negative component of the unipolar electrogram as a local procedural endpoint during paroxysmal atrial fibrillation catheter ablation using contact-force sensing: the UNIFORCE study. *J Interv Card Electrophysiol*. 2017;49(3):299-306. doi:10.1007/s10840-017-0264-4.
13. Das M, Loveday JJ, Wynn GJ, et al. Ablation index, a novel marker of ablation lesion quality: prediction of pulmonary vein reconnection at repeat electrophysiology study and regional differences in target values. *Europace*. May 2016. doi:10.1093/europace/euw105.
14. Calkins H, Hindricks G, Cappato R, et al. 2017 HRS/EHRA/ECAS/APHRS/SOLAECE expert consensus statement on catheter and surgical ablation of atrial fibrillation. *Heart Rhythm*. 2017;14(10):e275-e444. doi:10.1016/j.hrthm.2017.05.012.
15. Tomlinson DR. Derivation and validation of a VISITAG™-guided contact force ablation protocol for pulmonary vein isolation. *bioRxiv*. December 2017:232694. doi:10.1101/232694.

16. R: A language and environment for statistical computing. R Core Team, Foundation for Statistical Computing, Vienna, Austria. 2017:https://www.r-project.org/.
17. Irastorza RM, d'Avila A, Berjano E. Thermal latency adds to lesion depth after application of high-power short-duration radiofrequency energy: Results of a computer-modeling study. *J Cardiovasc Electrophysiol*. 2018;29(2):322-327. doi:10.1111/jce.13363.
18. Chelu MG, Morris AK, Kholmovski EG, et al. Durable lesion formation while avoiding esophageal injury during ablation of atrial fibrillation: Lessons learned from late gadolinium MR imaging. *J Cardiovasc Electrophysiol*. 2018;29(3):385-392. doi:10.1111/jce.13426.
19. Winkle RA, Moskovitz R, Hardwin Mead R, et al. Atrial fibrillation ablation using very short duration 50 W ablations and contact force sensing catheters. *J Interv Card Electrophysiol*. 2018;52(1):1-8. doi:10.1007/s10840-018-0322-6.
20. Arentz T, Weber R, Burkle G, et al. Small or Large Isolation Areas Around the Pulmonary Veins for the Treatment of Atrial Fibrillation?: Results From a Prospective Randomized Study. *Circulation*. 2007;115(24):3057-3063. doi:10.1161/CIRCULATIONAHA.107.690578.
21. Hutchinson MD, Garcia FC, Mandel JE, et al. Efforts to enhance catheter stability improve atrial fibrillation ablation outcome. *Heart Rhythm*. 2013;10(3):347-353. doi:10.1016/j.hrthm.2012.10.044.
22. Knecht S, Reichlin T, Pavlovic N, et al. Contact force and impedance decrease during ablation depends on catheter location and orientation: insights from pulmonary vein isolation using a contact force-sensing catheter. *J Interv Card Electrophysiol*. 2015;43(3):297-306. doi:10.1007/s10840-015-0002-8.
23. Chelu MG, Morris AK, Kholmovski EG, et al. Durable lesion formation while

avoiding esophageal injury during ablation of atrial fibrillation: Lessons learned from late gadolinium MR imaging. *J Cardiovasc Electrophysiol*. 2018;29(3):385-392. doi:10.1111/jce.13426.

24. Aizer A, Cheng A V., Wu PB, et al. Pacing Mediated Heart Rate Acceleration Improves Catheter Stability and Enhances Markers for Lesion Delivery in Human Atria During Atrial Fibrillation Ablation. *JACC Clin Electrophysiol*. 2018;4(4):483-490. doi:10.1016/j.jacep.2017.12.017.

## Tables

Table 1: Biophysical data at annotated sites of RF delivery at the LAPW according to ACCURESP™ setting (i.e. "on" versus "off") and site; data shown are mean [SD] or median ($1^{st}$ – $3^{rd}$ quartile), as appropriate.

Table 2: Annotated biophysical data at first-annotated LAPW sites according to ACCURESP™ setting (i.e. “on” versus “off”) and site; data shown are median ($1^{st}$ – $3^{rd}$ quartile).

Table 3: Annotated biophysical data at sites of deliberate catheter movement between first and second-annotated LAPW sites, identified according to criteria of a 0g CF event, or change in the UE morphology from pure R (site 1 completion) to RS (site 2 onset). RF duration, ILD, impedance drop and FTI data are displayed according to ACCURESP™ setting, with the difference (“Diff” – i.e. ACCURESP™ “on” minus “off”) also shown; PV, pulmonary vein.

Table 4: Difference in onset time of RF annotation during continuous RF at the LAPW; each site is calculated as annotation time for ACCURESP™ “on” minus “off”, with median ($1^{st}$ – $3^{rd}$ quartile, IQR), maximum and minimum differences shown.

| | Left-sided annotated sites | | | Right-sided annotated sites | | | All annotated sites | | |
|---|---|---|---|---|---|---|---|---|---|
| | ACCURESP ON | ACCURESP OFF | *p* | ACCURESP ON | ACCURESP OFF | *p* | ACCURESP ON | ACCURESP OFF | *p* |
| Total (N) | 5.4 [1.3] | 6.5 [1.6] | *0.15* | 4.9 [1.5] | 5.8 [1.7] | *0.28* | 5.1 [1.4] | 6.1 [1.6] | *0.07* |
| ILD (mm) | 5.6 [1.6] | 4.6 [1.7] | *0.01* | 6.2 [2.2] | 5.4 [2.6] | *0.16* | 6.0 (4.7 – 6.8) | 4.8 (3.9 – 5.6) | *0.002* |
| RF duration (s) | 13.1 [4.4] | 9.9 [3.9] | *0.0003* | 13.5 [5.5] | 10.6 [3.9] | *0.006* | 13.3 (10.3 – 15.6) | 10.6 (7.5 – 13.2) | *<0.0001* |
| Mean CF (g) | 12.1 (9.9 – 15.6) | 11.5 (9.7 – 14.9) | *0.67* | 17.9 (13.4 – 21.6) | 18.6 (12.1 – 22.1) | *0.68* | 14.4 (10.8 – 19.7) | 14.0 (10.7 – 19.9) | *0.85* |
| Impedance drop (Ω) | 8.0 (4.3 – 12.2) | 6.6 (3.4 – 10.6) | *0.24* | 5.9 (1.5 – 8.8) | 3.7 (0.8 – 7.1) | *0.34* | 6.5 (3.5 – 10.0) | 5.4 (1.7 – 8.9) | *0.14* |
| FTI (g.s) | 156 (123 – 204) | 114 (31 – 161) | *0.0003* | 228 (134 – 315) | 166 (111 – 243) | *0.04* | 177 (133 – 250) | 130 (104 – 195) | *0.0002* |

Table 1

| | **Left-sided 1st annotated site** | | | **Right-sided 1st annotated site** | | | **All 1st annotated sites** | | |
|---|---|---|---|---|---|---|---|---|---|
| | ACCURESP ON | ACCURESP OFF | *p* | ACCURESP ON | ACCURESP OFF | *p* | ACCURESP ON | ACCURESP OFF | *p* |
| Distance to site 2 (mm) | 6.6 (6.3 – 7.0) | 5.3 (4.6 – 6.3) | *0.05* | 7.2 (6.3 – 8.4) | 5.0 (4.5 – 8.1) | *0.04* | 6.7 (6.3 – 7.8) | 5.2 (4.5 – 6.8) | *0.005* |
| RF duration (s) | 16.0 (15.2 – 18.7) | 15.1 (14.7 – 15.6) | *0.08* | 15.5 (14.7 – 23.7) | 15.1 (14.7 – 15.7) | *0.20* | 15.7 (14.9 – 22.2) | 15.1 (14.7 – 15.6) | *0.02* |
| Mean CF (g) | 10.8 (9.5 – 12.9) | 10.8 (9.0 – 13.0) | *0.84* | 16.8 (12.6 – 21.6) | 17.8 (11.7 – 21.2) | *0.84* | 12.9 (10.1 – 18.2) | 13.0 (9.0 – 18.3) | *0.56* |
| Impedance drop (Ω) | 13.5 (11.5 – 23.6) | 13.5 (10.9 – 21.5) | *0.06* | 10.3 (8.5 – 12.4) | 10.3 (7.8 – 12.4) | *1.00* | 12.0 (9.1 – 15.7) | 11.5 (9.1 – 15.2) | *0.03* |
| FTI (gs) | 185 (150 - 230) | 163 (123 - 198) | *0.11* | 268 (240 - 376) | 264 (185 - 327) | *0.16* | 240 (163 - 322) | 198 (135 - 270) | *0.02* |

Table 2

| Case number | PV | Position instability criterion | Site 1 RF duration (s) | | | Distance to site 2 (mm) | | | Site 1 impedance drop (Ω) | | | Site 1 FTI (g.s) | | |
|---|---|---|---|---|---|---|---|---|---|---|---|---|---|---|
| | | | ACCURESP | | | ACCURESP | | | ACCURESP | | | ACCURESP | | |
| | | | ON | OFF | *Diff* | ON | OFF | *Diff* | ON | OFF | *Diff* | ON | OFF | *Diff* |
| 5 | Right | 0g CF | 15.5 | 15.6 | *-0.1* | 6.3 | 4.1 | *2.2* | 9.4 | 9.4 | *0* | 228 | 228 | *0* |
| 10 | Right | 0g CF | 14.4 | 14.4 | *0* | 8.6 | 7.8 | *0.8* | 25.3 | 25.3 | *0* | 261 | 261 | *0* |
| 11 | Right | 0g CF | 14.0 | 14.6 | *-0.6* | 8.6 | 6.5 | *2.1* | 6.5 | 6.5 | *0* | 382 | 399 | *-17* |
| 5 | Left | Pure R UE to RS | 26.5 | 15.2 | *11.3* | 6.7 | 4.1 | *2.6* | 29.5 | 26.2 | *3.3* | 256 | 117 | *139* |
| 11 | Left | Pure R UE to RS | 20.9 | 18.6 | *2.3* | 4.9 | 5.2 | *-0.3* | 12.2 | 11.1 | *1.1* | 482 | 434 | *48* |
| 22 | Right | Pure R UE to RS | 15.1 | 14.8 | *0.3* | 6.1 | 5.0 | *1.1* | 11.1 | 11.1 | *0* | 274 | 272 | *2* |
| 23 | Right | Pure R UE to RS | 15.5 | 15.0 | *0.5* | 8.1 | 8.8 | *-0.7* | 11.9 | 11.9 | *0* | 120 | 112 | *8* |

Table 3

| **Annotated site number** | **Left-sided annotation onset difference (s)** | | | **Right-sided annotation onset difference (s)** | | |
|---|---|---|---|---|---|---|
| | *Median (IQR)* | *Maximum* | *Minimum* | *Median (IQR)* | *Maximum* | *Minimum* |
| 2 | 1.2 (0.4 – 5.0) | 11.3 | -1.3 | 0.3 (-0.02 – 8.0) | 8.6 | -0.02 |
| 3 | 7.3 (4.4 – 10.8) | 16.3 | 0.7 | 4.2 (-0.04 – 10.8) | 11.9 | -0.04 |
| 4 | 11.6 (6.3 – 14.4) | 19.5 | 0.02 | -0.04 (-0.9 – 6.9) | 13.4 | -1.7 |
| 5 | 14.6 (7.6 – 23.0) | 28.2 | 2.1 | 2.5 (0.8 – 11.9) | 15.6 | -0.06 |

Table 4

## Figures

Figure 1: Reconstituted curves from VISITAG™ Module data export demonstrating first-annotated site "end" time-point at the first 0g CF event, 15.5s (ACCURESP™ "on") and 15.6s (ACCURESP™ "off") following RF onset in case 5, right PV. This small difference in the annotated RF duration between ACCURESP™ settings results in a single vertical red line representing ACURESP™ "on" and "off" annotation timing. Catheter tip position shift, (position) standard deviation (SD), CF and impedance are plotted separately; x-axis displays the PIU time stamp (i.e. running case time, shown in thousands of seconds) and vertical dashed lines indicate end-expiration time-points. The force-over-time 100% minimum 1g CF filter ensures that automated RF annotation only occurs when CF is continuously maintained ≥1g, indicated by black curves; pink position shift, SD and impedance curves indicate <100% CF filter preference attainment. The SD curve returns to black at 1s (or 60 sites) following attainment of both CF and position stability within the chosen VISITAG™ Module filter preferences, in view of the CARTO®3 SD calculation "system logic".

Figure 2: Reconstituted curves from VISITAG™ Module data export demonstrating first-annotated site "end" time-point at the first 0g CF event, 14.4s following RF onset in case 10, right PV. This small difference in the annotated RF duration between ACCURESP™ settings results in a single vertical red line representing ACURESP™ "on" and "off" annotation timing; other plot elements are as per figure 1.

Figure 3: Reconstituted curves from VISITAG™ Module data export demonstrating first-annotated site "end" time-point at the first 0g CF event, 14.0s (ACCURESP™ "on", red line)

and 14.6s (ACCURESP™ “off”, blue line) following RF onset in case 11, right PV; other plot elements are as per figure 1.

Figure 4: Reconstituted curves from VISITAG™ Module data export demonstrating first-annotated site “end” time-point at 15.2s (ACCURESP™ “off”, blue line) and 26.5s (ACCURESP™ “on”, red line) following RF onset in case 5, left PV. Transition to site 2 with ACCURESP “off” coincided with UE morphology change from pure R at site 1 completion, to RS at site 2 onset (ACCURESP™ “off” ILD 4.1mm); clear changes in the catheter tip position shift, (position) standard deviation (SD) and CF coincide with ACCURESP™ “off” annotation. All curves are drawn black, since CF was maintained ≥1g and the catheter movement was sufficiently rapid to ensure that all catheter tip location data was annotated to either site 1, or 2 (ACCURESP™ “off”).

Figure 5: Reconstituted curves from VISITAG™ Module data export demonstrating first-annotated site “end” time-point at 18.6s (ACCURESP™ “off”, blue line) and 20.9s (ACCURESP™ “on”, red line) following RF onset in case 11, left PV. Transition to site 2 with ACCURESP “off” coincided with UE morphology change from pure R at site 1 completion, to RS at site 2 onset (ACCURESP™ “off” ILD 5.2mm). The greatest position shift value is seen occurring closest to ACCURESP™ “off” annotation timing; other plot elements are as per figure 4.

Figure 6: Reconstituted curves from VISITAG™ Module data export demonstrating first-annotated site “end” time-point at 14.8s (ACCURESP™ “off”, blue line) and 15.1s

(ACCURESP™ “on”, red line) following RF onset in case 22, right PV. Transition to site 2 with ACCURESP “off” coincided with UE morphology change from pure R at site 1 completion, to RS at site 2 annotation onset (ACCURESP™ “off” ILD 5.0mm); clear changes in the catheter tip position shift and (position) standard deviation (SD) occur just before ACCURESP™ “off” annotation. All curves are drawn black, since CF was maintained ≥1g and the catheter movement was sufficiently rapid to ensure that all catheter tip location data was annotated to either site 1, or 2 (ACCURESP™ “off”).

Figure 7: Reconstituted curves from VISITAG™ Module data export demonstrating first-annotated site “end” time-point at 15.0s (ACCURESP™ “off”, blue line) and 15.5s (ACCURESP™ “on”, red line) following RF onset in case 23, right PV. Transition to site 2 with ACCURESP “off” coincided with UE morphology change from pure R at site 1 completion, to RS at site 2 annotation onset (ACCURESP™ “off” ILD 8.8mm); the first obvious changes in the catheter tip position shift, (position) standard deviation (SD) and CF coincide with ACCURESP™ “off” annotation. The curves are briefly shown in pink since with ACCURESP™ “off” there was 0.28s of non-annotated inter-ablation site transition time due position instability >2*(2mm SD) according to the CARTO®3 “system logic”; the position SD curve is pink for a total of 1.28s, reflecting system SD calculations over a minimum of 60 positions (i.e. 1s).

Figure 8: ACCURESP™ “on” minus “off” difference in annotated RF duration, FTI and impedance drop according to site 1-2 inter-ablation site distance with ACCURESP™ “off”. Data are shown for all 13 LAPW inter-ablation site transitions achieved during constant catheter-tissue contact.

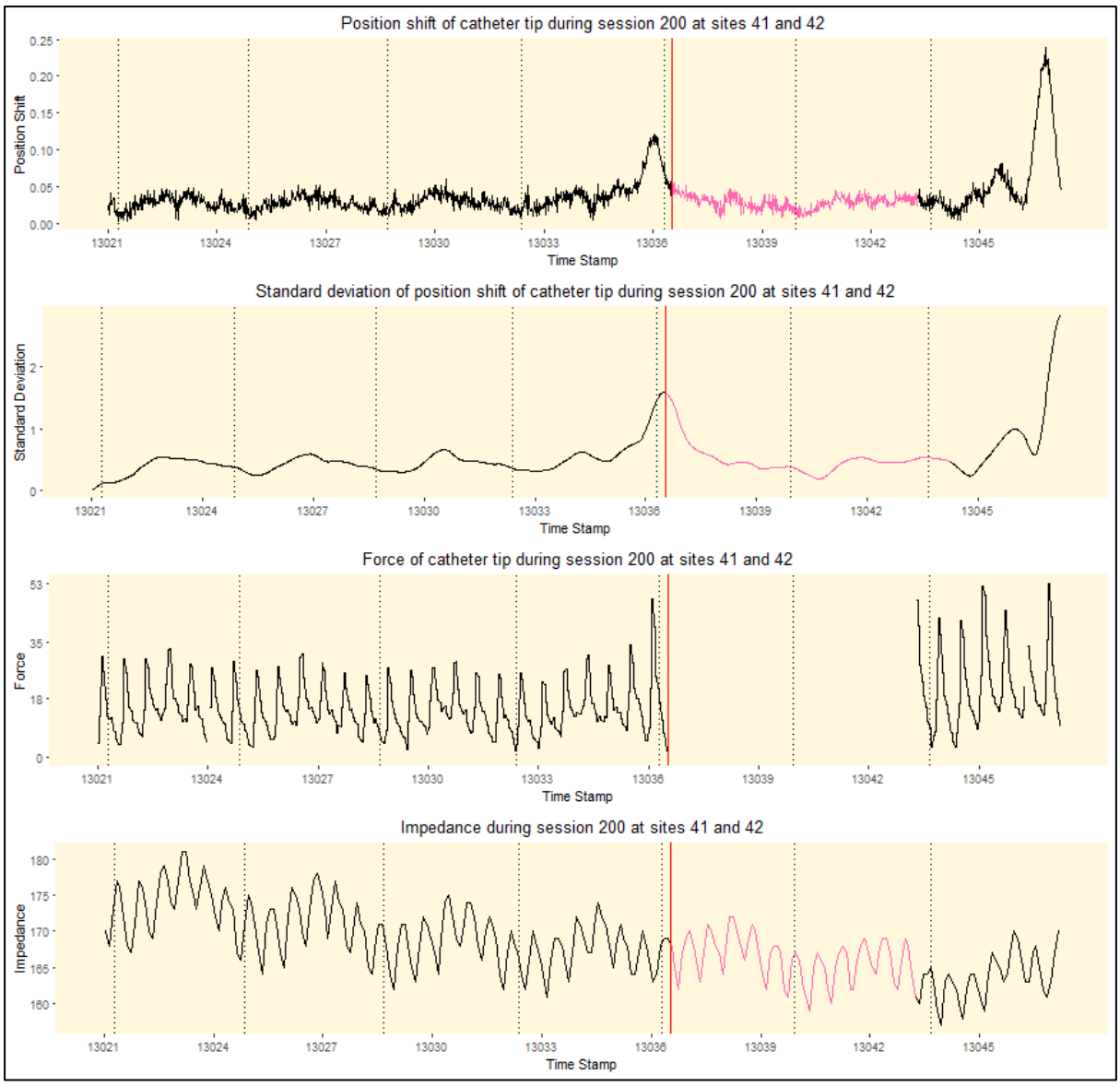
Position shift of catheter tip during session 200 at sites 41 and 42
Position Shift
0.25
0.20
0.15
0.10
0.05
0.00
13021
13024
13027
13030
13033
13036
13039
13042
13045
Time Stamp
Standard deviation of position shift of catheter tip during session 200 at sites 41 and 42
Standard Deviation
2
1
0
Time Stamp
Force of catheter tip during session 200 at sites 41 and 42
Force
53
35
18
0
Time Stamp
Impedance during session 200 at sites 41 and 42
Impedance
180
175
170
165
160
Time Stamp

Figure 1

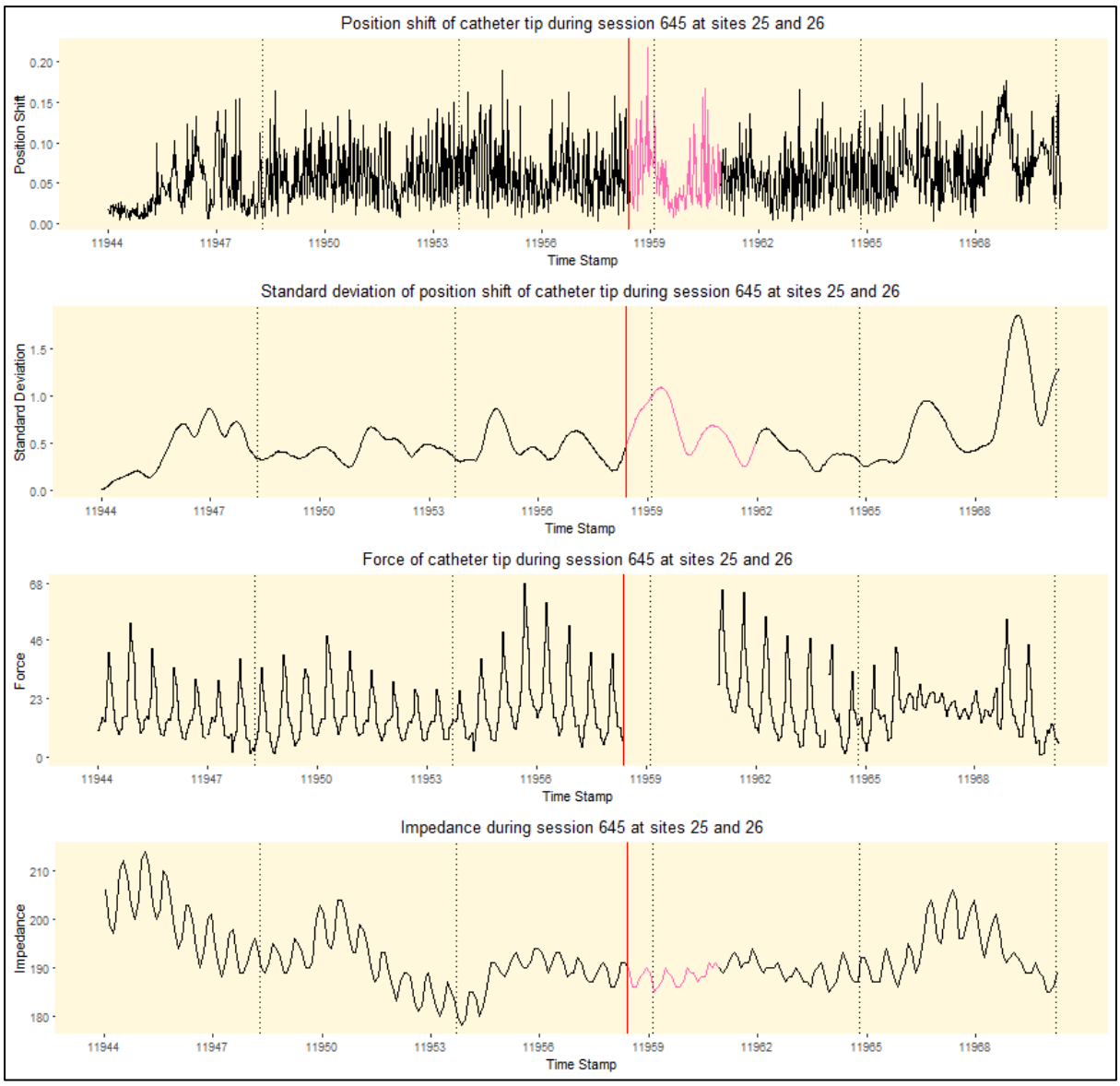
Position shift of catheter tip during session 645 at sites 25 and 26
Position Shift
0.20
0.15
0.10
0.05
0.00
11944
11947
11950
11953
11956
11959
11962
11965
11968
Time Stamp
Standard deviation of position shift of catheter tip during session 645 at sites 25 and 26
Standard Deviation
1.5
1.0
0.5
0.0
Time Stamp
Force of catheter tip during session 645 at sites 25 and 26
Force
68
46
23
0
Time Stamp
Impedance during session 645 at sites 25 and 26
Impedance
210
200
190
180
Time Stamp

Figure 2


Position shift of catheter tip during session 707 at sites 35 and 36
Position Shift
0.0
0.1
0.2
8659
8663
8667
8671
8675
8679
8683
8687
8691
8695
Time Stamp
Standard deviation of position shift of catheter tip during session 707 at sites 35 and 36
Standard Deviation
0
1
2
Time Stamp
Force of catheter tip during session 707 at sites 35 and 36
Force
0
21
42
64
Time Stamp
Impedance during session 707 at sites 35 and 36
Impedance
170
175
180
Time Stamp

Figure 3

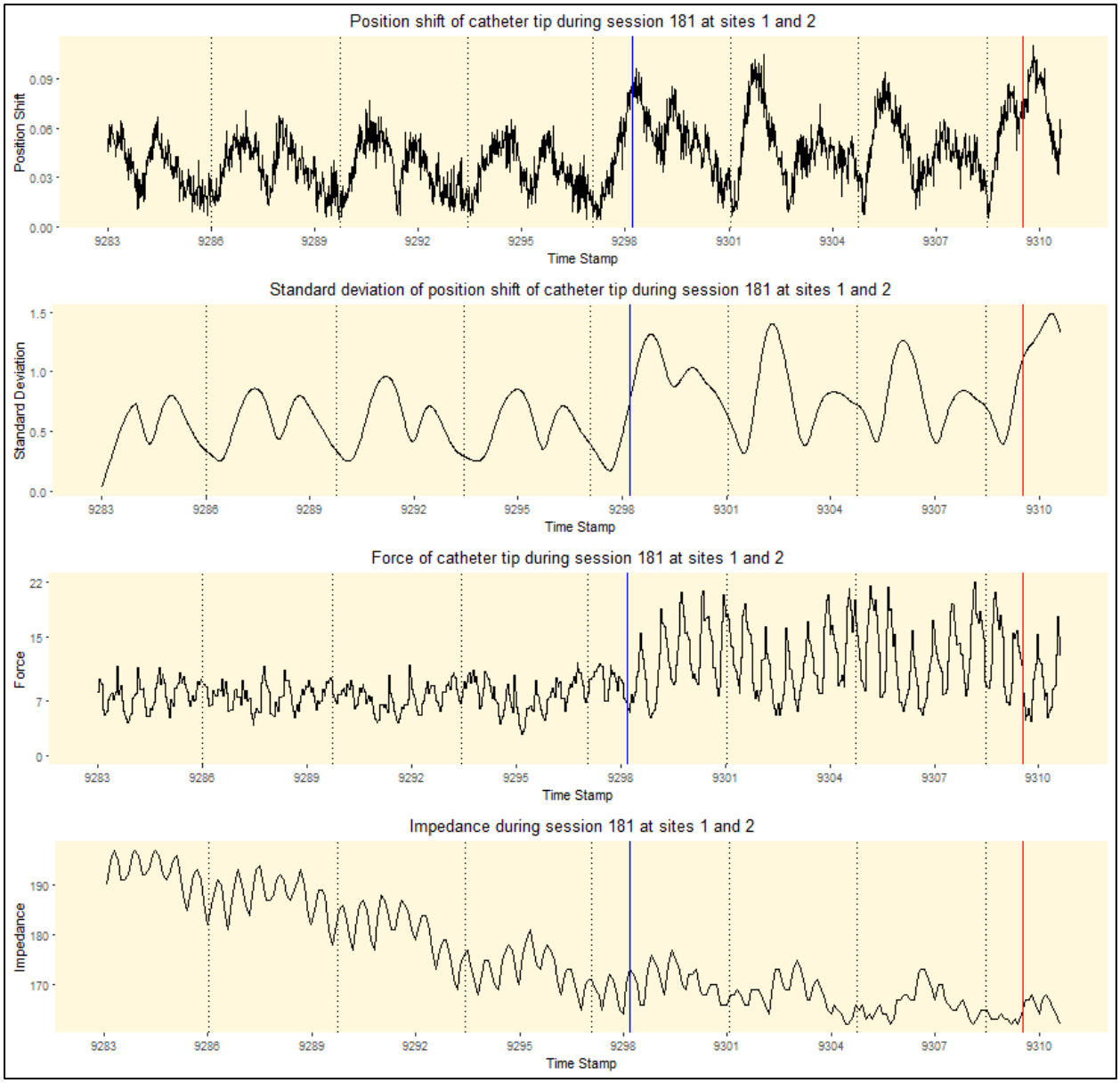
Position shift of catheter tip during session 181 at sites 1 and 2
Position Shift
0.00
0.03
0.06
0.09
9283
9286
9289
9292
9295
9298
9301
9304
9307
9310
Time Stamp
Standard deviation of position shift of catheter tip during session 181 at sites 1 and 2
Standard Deviation
0.0
0.5
1.0
1.5
Time Stamp
Force of catheter tip during session 181 at sites 1 and 2
Force
0
7
15
22
Time Stamp
Impedance during session 181 at sites 1 and 2
Impedance
170
180
190
Time Stamp

Figure 4

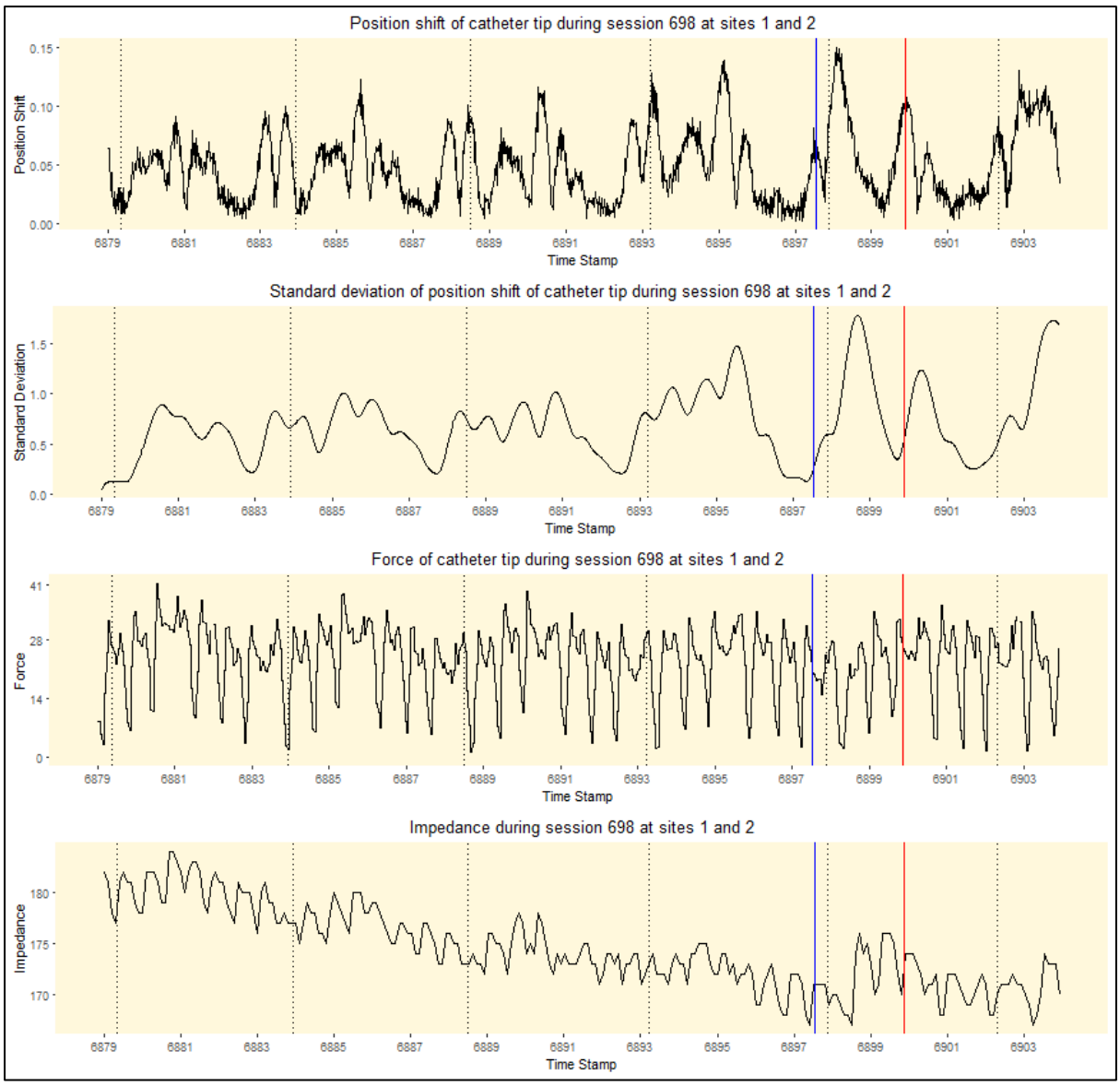
Position shift of catheter tip during session 698 at sites 1 and 2
Position Shift
0.15
0.10
0.05
0.00
6879
6881
6883
6885
6887
6889
6891
6893
6895
6897
6899
6901
6903
Time Stamp
Standard deviation of position shift of catheter tip during session 698 at sites 1 and 2
Standard Deviation
1.5
1.0
0.5
0.0
Time Stamp
Force of catheter tip during session 698 at sites 1 and 2
Force
41
28
14
0
Time Stamp
Impedance during session 698 at sites 1 and 2
Impedance
180
175
170
Time Stamp

Figure 5

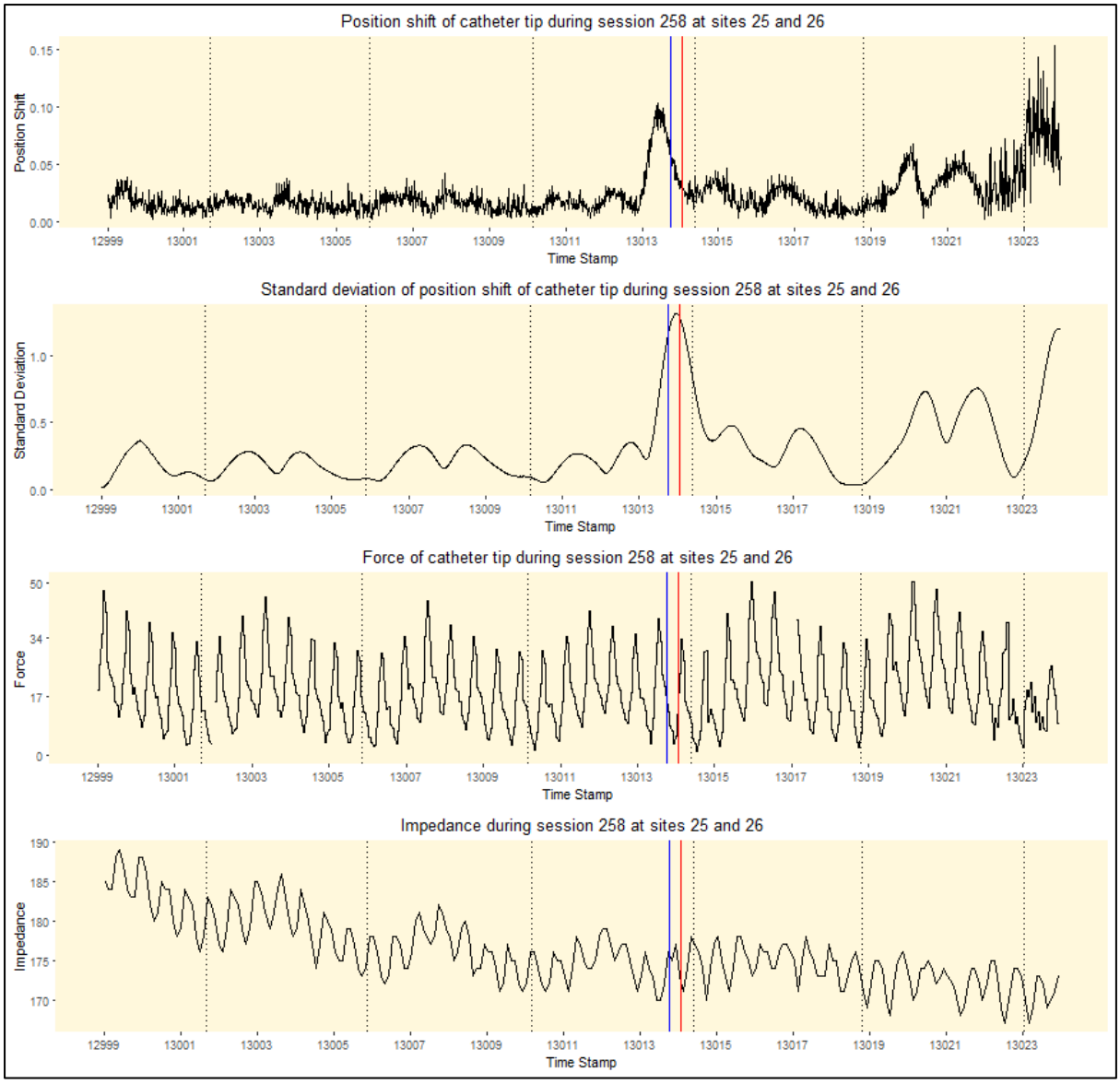
Position shift of catheter tip during session 258 at sites 25 and 26
Position Shift
0.15
0.10
0.05
0.00
12999
13001
13003
13005
13007
13009
13011
13013
13015
13017
13019
13021
13023
Time Stamp
Standard deviation of position shift of catheter tip during session 258 at sites 25 and 26
Standard Deviation
1.0
0.5
0.0
Time Stamp
Force of catheter tip during session 258 at sites 25 and 26
Force
50
34
17
0
Time Stamp
Impedance during session 258 at sites 25 and 26
Impedance
190
185
180
175
170
Time Stamp

Figure 6

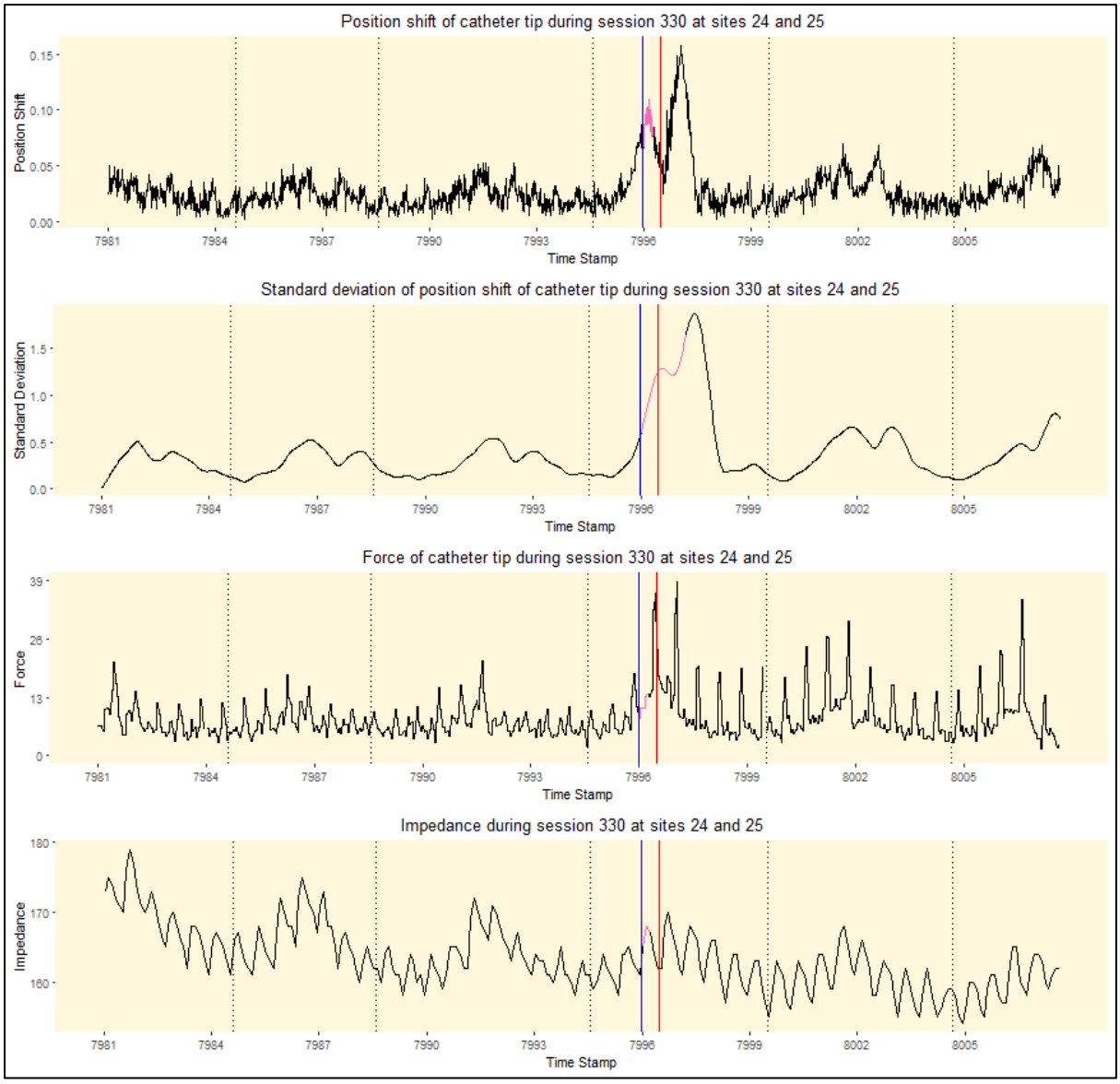
Position shift of catheter tip during session 330 at sites 24 and 25
Position Shift
0.15
0.10
0.05
0.00
7981
7984
7987
7990
7993
7996
7999
8002
8005
Time Stamp
Standard deviation of position shift of catheter tip during session 330 at sites 24 and 25
Standard Deviation
1.5
1.0
0.5
0.0
Time Stamp
Force of catheter tip during session 330 at sites 24 and 25
Force
39
26
13
0
Time Stamp
Impedance during session 330 at sites 24 and 25
Impedance
180
170
160
Time Stamp

Figure 7

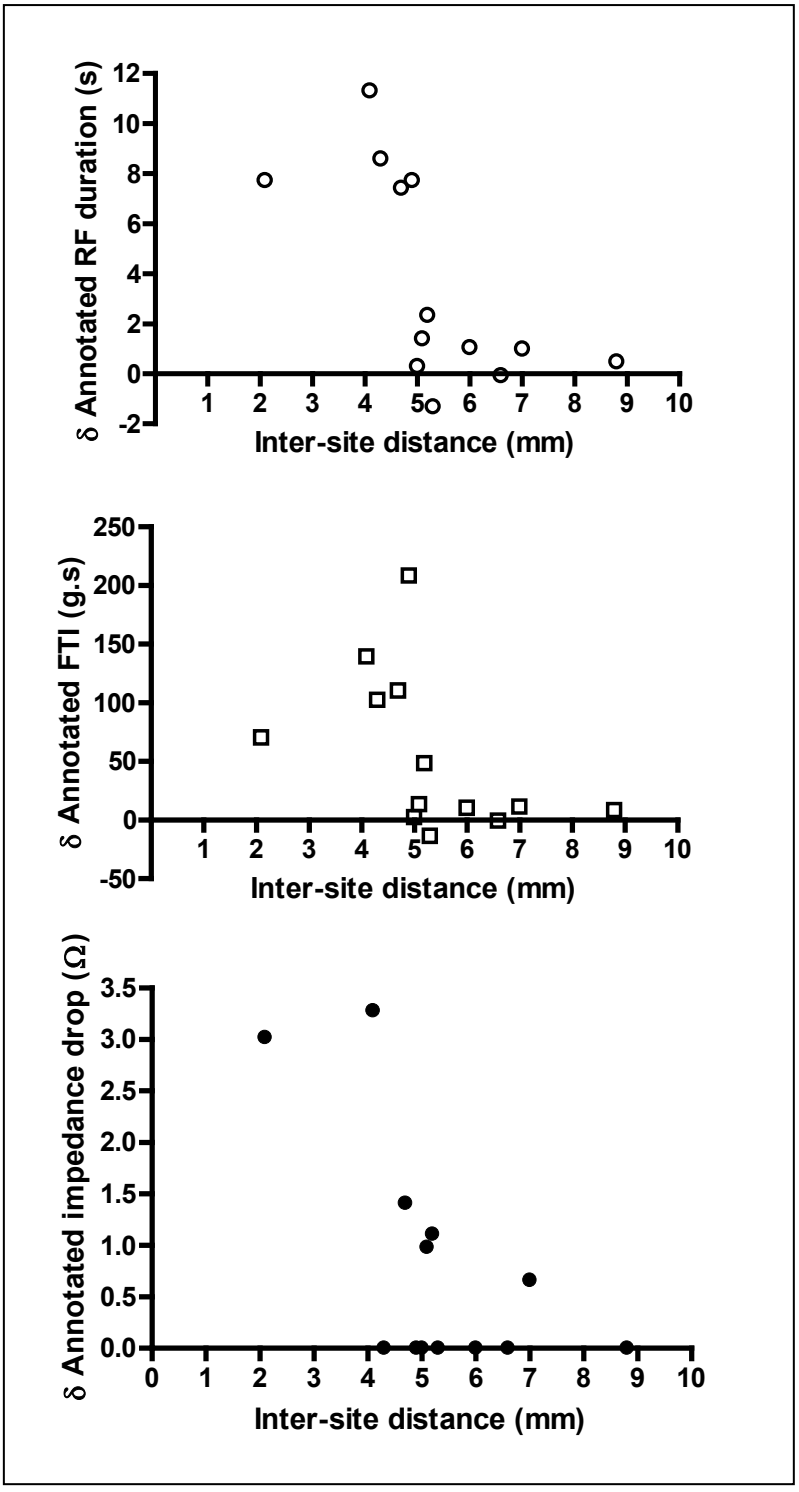
δ Annotated RF duration (s)
12
10
8
6
4
2
0
-2
1 2 3 4 5 6 7 8 9 10
Inter-site distance (mm)
δ Annotated FTI (g.s)
250
200
150
100
50
0
-50
1 2 3 4 5 6 7 8 9 10
Inter-site distance (mm)
δ Annotated impedance drop (Ω)
3.5
3.0
2.5
2.0
1.5
1.0
0.5
0.0
0 1 2 3 4 5 6 7 8 9 10
Inter-site distance (mm)

Figure 8